Available online at www.sciencedirect.com
SCIENCE DIRECT
Catalysis Today 104 (2005) 154–159
CATALYSIS TODAY
www.elsevier.com/locate/cattod

Partial oxidation of methane in $Ba_{0.5}Sr_{0.5}Co_{0.8}Fe_{0.2}O_{3-\delta}$ membrane reactor at high pressures

Hui Lu, Jianhua Tong, You Cong, Weishen Yang *

State Key Laboratory of Catalysis, Dalian Institute of Chemical Physics, Chinese Academy of Science, P.O. Box 110, Dalian 116023, PR China

Available online 4 May 2005

Abstract

Oxygen permeation fluxes through dense disk-shaped $Ba_{0.5}Sr_{0.5}Co_{0.8}Fe_{0.2}O_{3-\delta}$ (BSCFO) membranes were investigated as a function of temperature (973–1123 K), pressure (2–10 atm), and membrane thickness (1–2 mm) under an air/helium gradient. A high oxygen permeation flux of 2.01 ml/cm^2 min was achieved at 1123 K and 10 atm under an air/He oxygen partial pressure gradient. Based on the dependence of the oxygen permeation flux on the oxygen partial pressure difference across the membrane and the membrane thickness, it is assumed that bulk diffusion of oxygen ions was the rate-controlling step in the oxygen transport across the BSCFO membrane disk under an air/He gradient. The partial oxidation of methane (POM) to syngas using $LiLaNiO_x/\gamma$-Al_2O_3 as catalyst in a BSCFO membrane reactor was successfully performed at high pressure (5 atm). Ninety-two percent methane conversion, 90% CO selectivity, and 15.5 ml/cm^2 min oxygen permeation flux were achieved in steady state at a temperature of 1123 K and a pressure of 5 atm. A syngas production rate of ~79 ml/cm^2 min was obtained. Characterization of the membrane surface by SEM and XRD after reaction showed that the surface exposed to the air side preserved the Perovskite structure while the surface exposed to the reaction side was eroded.

Keywords: Mixed-conducting ceramic membrane; POM; Oxygen separation; Membrane reactor; Perovskite

1. Introduction

Economical uses of natural gas have attracted extensive attention all over the world [1]. Due to the fact that the transport cost of natural gas rapidly rises with increasing distance, gas-to-liquid (GTL) processes have received considerable attention during the past decade, because the most economical use of natural gas seems to be conversion into value-added liquid chemical products at the site of the gas source. During the past years, extensive efforts have been performed on both direct (oxidative coupling of methane to ethane and ethylene, selective oxidation of methane to methanol and formaldehyde) and indirect conversion of methane (reforming of methane to syngas, and then producing a series of important chemical products such as liquid fuels and methanol) [1–6]. In direct conversion the reaction products are easily further oxidized to CO_2 and H_2O because they are more reactive than the starting materials, which leads to a low selectivity to the target products. At present, the use of natural gas in the chemical industry therefore is mainly through the indirect conversion route, where natural gas to syngas is the first step of the application.

It is well known that partial oxidation of methane (POM) to syngas holds great promise, and probably is able to replace steam reforming of methane (SRM) and CO_2 reforming of methane for the production of syngas. For the latter two reactions, due to the strong endothermicity and the slow reaction rate, more energy supply and higher plant investment are required. POM is mildly exothermic and can produce syngas with a H_2/CO molar ratio of 2/1, which can be directly used as a feed for methanol synthesis or Fischer–Tropsch (F–T) reaction. However, F–T synthesis cannot tolerate nitrogen, so pure oxygen is required [2]. Oxygen permeable membranes made from mixed ionic and electronic conductors have potential applications in the

* Corresponding author. Tel.: +86 411 84379073; fax: +86 411 84694447.
E-mail address: yangws@dicp.ac.cn (W. Yang).
URL: http://yanggroup.dicp.ac.cn

0920-5861/$ – see front matter © 2005 Elsevier B.V. All rights reserved.
doi:10.1016/j.cattod.2005.03.078

separation of pure oxygen from air and as membrane reactors for light hydrocarbon conversion [2–6]. Using air as the most economical oxygen source, a dense oxygen-permeable membrane reactor can be applied to POM to syngas, moreover it can also be used to produce pure oxygen from oxygen-containing gas. Coupling POM with an oxygen permeation membrane could allow for the separation of oxygen and the catalytic oxidation in one unit, so the heat produced by POM could maintain the temperature needed for oxygen separation, resulting in a reduction of GTL production cost by 20–30% [7–8]. In literature several materials, e.g. $SrCo_{0.5}FeO_{3.25-\delta}$ and $La_{0.2}Ba_{0.8}Co_{0.2}Fe_{0.8}O_{3-\delta}$, have been used in POM membrane reactors in the temperature range of 1123–1223 K at atmospheric pressure [3,9–13]. However, with respect to energy savings, plant investment cost, and the synthesis of the downstream products, it would be much better to operate the POM in an oxygen-permeable membrane reactor at high pressure.

Mixed-conducting Perovskite-type oxides have considerably high oxygen ionic conductivity with overwhelming electronic conductivity at elevated temperatures, and usually high oxygen permeation fluxes are found for such materials [13–15]. However, for practical application the oxygen-permeable membranes must possess sufficiently high oxygen permeability and structural stability to withstand harsh conditions (syngas atmosphere, carbon dioxide, etc.). Attracted by the high oxygen permeation flux of $SrCo_{0.8}Fe_{0.2}O_{3-\delta}$ (SCFO), the properties of the membrane such as surface exchange kinetics, electrical conductivity, oxygen non-stoichiometry, phase structure stability and oxygen permeability have been investigated extensively [13–15]. Unfortunately, the poor chemical and structural stability of SCFO in reducing environments limits its practical application [16–18]. The substitution of the A-site strontium in SCFO with higher valence state metal ions (such as lanthanum) can lead to an improvement in phase stability, but the oxygen permeability is lowered due to the decrease of the oxygen vacancy concentration [17]. B-site ion substituted (for example, by Zr^{4+} and $Ce^{3/4+}$) membranes based on $BaFe(Co)O_{3-\delta}$ were developed recently, and the structural stability of these novel materials was improved greatly [13,18–20], but the oxygen permeability was significantly lower because of the reduced oxygen vacancy concentration and ionic conductivity. However, by proper substitution of Sr^{2+} in SCFO by Ba^{2+} having a larger ionic radius, its structural stability was improved significantly and the oxygen permeation flux was also increased [2,4,18].

In our research group, we developed some oxygen permeation membrane materials with high oxygen permeation performance and good structural stability, e.g. $Ba_{0.5}Sr_{0.5}Co_{0.8}Fe_{0.2}O_{3-\delta}$ (BSCFO), $BaCo_{0.4}Fe_{0.4}Zr_{0.2}O_{3-\delta}$ (BCFZO), and applied these materials to POM for production of synthesis gas at atmospheric pressure [2,13]. The purpose of the present study is to investigate the oxygen permeability of the BSCFO membrane material under air/helium gradient and the POM in a BSCFO membrane reactor at high pressure.

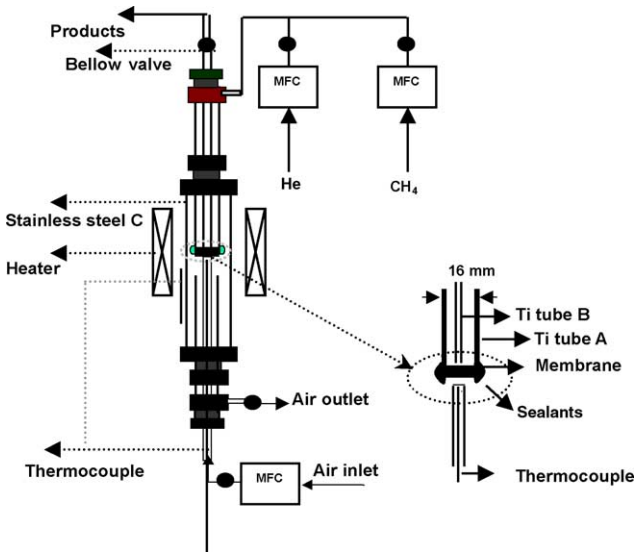

Fig. 1. Membrane reactor assembly for POM at high pressure.

2. Experimental

BSCFO powder was prepared by a combined EDTA–citric acid complexation method. The as-prepared oxide was pressed into a disk pellet in a stainless steel mold under a hydraulic pressure of 15–20 MPa. The green disk was sintered at 1423 K for 3–5 h at static air, and then cooled to ambient temperature. Details of the preparation were described previously [2]. A $LiLaNiO_x/\gamma\text{-}Al_2O_3$ catalyst with 10 wt.% nickel loading was prepared by an impregnation method [2,13], namely, impregnating appropriate amounts of $LiNO_3$, $Ni(NO_3)_2$ and $La(NO_3)_3$ on $\gamma\text{-}Al_2O_3$ supports for 24 h, drying at 393 K, and then calcining in air at 873–1073 K for 4 h [2,13].

The experimental apparatus and the membrane reactor configuration are presented in Fig. 1. In the membrane reactor, the BSCFO membrane disk was sealed on the bottom of a Ti-tube A by using two special inorganic sealing materials. Another Ti-tube B was inserted into the Ti-tube A as an outlet for the products. The Ti-tube A was housed by another SS-tube C to get a high-pressure membrane reactor. Two thermocouples were used for controlling and measuring the temperatures of the electrical furnace and the membrane disk. For oxygen permeation measurements under an air/helium gradient, one side of the membrane was exposed to air (150 ml/min), while the other side was exposed to helium (10 ml/min). For POM in the membrane reactor, one side of the membrane was exposed to air (250 ml/min), while the other side was exposed to a mixture of methane diluted with He. Before reaction, the unreduced catalyst particles of $LiLaNiO_x/\gamma\text{-}Al_2O_3$ (0.3 g) were packed on the surface of the membrane, and the temperature of membrane reactor was

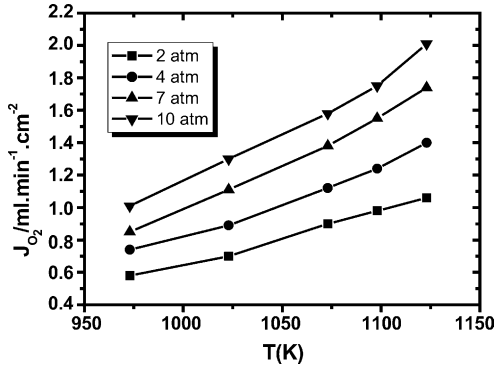

Fig. 2. Oxygen permeation fluxes of the BSCFO membrane as a function of temperature at different pressure.

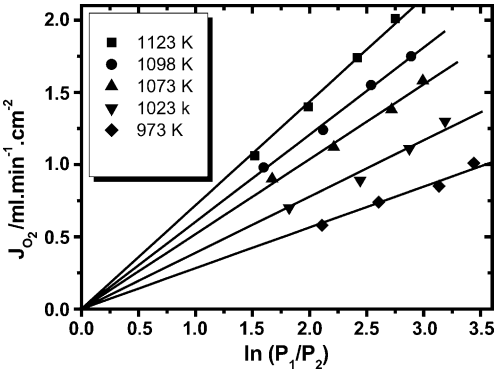

Fig. 3. Dependence of the oxygen permeation flux through the BSCFO membrane on $\ln(P_2/P_1)$ at different temperatures.

increased to 1123 K at a rate of 0.5 K/min. An on-line gas chromatograph (HP 6890 Plus) equipped with a thermal conductivity detector and an auto-sampling valve was used to analyze the products. A 13X molecular sieve column and a Porapak Q column were used to separate the products for analysis.

After the reaction, the crystal phases of the membrane were determined by XRD (Miniflex, Rigaku, Japan) using Cu Kα radiation (0.1542 nm) at 30 kV × 15 mA and a scanning speed of 8°/min from 10° to 80° with steps of 0.02°. The membrane surface morphology was examined by scanning electron microscopy (SEM, JEM-1200, Japan).

3. Results and discussion

The dependence of the oxygen permeation flux through the $Br_{0.5}Sr_{0.5}CO_{0.8}Fe_{0.2}$ (BSCFO) membrane on temperature at different pressures is shown in Fig. 2. The BSCFO membrane material shows a very high oxygen permeability in the range of temperatures and pressures investigated. As show in Fig. 2, the oxygen permeation flux increases with increasing of temperature and pressure because the oxygen ion diffusion rate in the bulk lattice is driven by the pressure difference and the surface oxygen and oxygen ion exchange rates are accelerated by temperature. For example, the oxygen permeation flux reaches 1.05 ml/cm^2 min at 1123 K under an air/He gradient at 2 atm, and increases to 2.01 ml/cm^2 min at 10 atm, which is higher than the oxygen permeation value (1.0 ml/cm^2 min) specified by Steele [21,22] for industrial application. The activation energy of oxygen permeation (calculated based on Fig. 2) at different pressures is almost the same. The average value is 39.4 kJ/mol, which is close to the value at atmospheric pressure, 40.8 kJ/mol [4].

Mixed-conducting oxygen permeable membranes represent a class of ceramic membranes, which exhibit both oxygen ionic and electronic conductivity. By applying an oxygen partial pressure gradient across the membrane, oxygen is driven from the high partial pressure side to the low partial pressure side. Local charge neutrality is maintained by joint diffusion of oxygen vacancies and electrons or electron holes. Mixed conduction involves simultaneous transport of both ionic and electronic charge carriers in presence of an oxygen potential gradient. Oxygen ions will be transported through the material without the need for external electrodes. In general, the oxygen transport can be described by two processes: the surface exchange reactions on the membrane surfaces and the ionic diffusion through the bulk material. If the controlling step of oxygen permeation is bulk diffusion, the oxygen permeation flux (J_{O_2}) of the membrane can be described as follows [23]:

$$J_{O_2} = \frac{RT}{16F^2L}\left(\frac{\sigma_i\sigma_e}{\sigma_i+\sigma_e}\right)\ln\left(\frac{P_2}{P_1}\right) \quad (1)$$

where L (cm) is the membrane thickness, P_1 (atm) and P_2 (atm) are the low and high oxygen partial pressures on both sides of the membrane respectively. σ_i and σ_e (S cm^{-1}) denote the oxygen ion and electron conductivity of the membrane material, respectively. The other symbols have their original meanings.

Eq. (1) predicts that if oxygen permeation is controlled by bulk diffusion, the oxygen permeation flux should be linearly proportional to the pressure term $\ln(P_2/P_1)$ and the reciprocal of the membrane thickness ($1/L$). Fig. 3 shows a plot of the oxygen permeation flux against $\ln(P_2/P_1)$. It can be seen that there is a good linear relationship between the oxygen permeation flux and $\ln(P_2/P_1)$ in the temperature range of 973–1123 K. At atmospheric pressure, the dependence of the oxygen permeation flux on the thickness was studied previously [18,24]. It was found that the oxygen permeation flux increased with decreasing membrane thickness, i.e., it was linearly proportional to the reciprocal of the membrane thickness ($1/L$). For high pressure, we measured the oxygen permeation fluxes of the disk membranes with different thicknesses in the temperature range of 973–1123 K at 4 atm. The measured oxygen permeation flux as a function of $1/L$ is shown in Fig. 4. It can be seen that the oxygen permeation flux is also linearly proportional to $1/L$ at constant temperature. These results

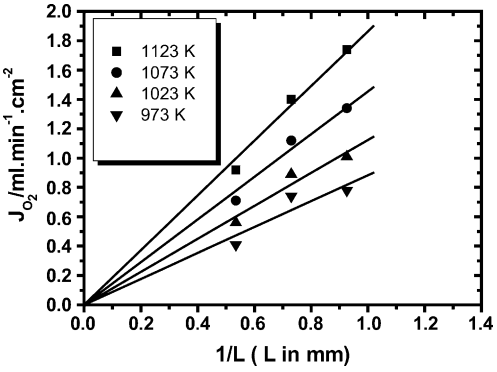

Fig. 4. Dependence of the oxygen permeation flux through the BSCFO membrane on 1/*L* at different temperatures (*P* = 4 atm).

suggest that the oxygen permeation process is controlled by bulk diffusion also under high-pressure conditions.

The blank catalytic behavior for methane conversion of the BSCFO membrane sealed on the Ti tube was studied without catalyst at 1123 K under atmospheric pressure. After the membrane was sealed on the Ti-tube at high temperature, air (outside) and diluted methane (inside) were supplied to each side of the BSCFO membrane reactor, respectively. The products detected in the gas eluted from the reaction chamber were CO, CO_2, H_2O, H_2 and O_2, but no C_2 products were found. With an increase of the flow rate of diluted methane (25% methane diluted with helium, 40–100 ml/min), methane conversion decreases from 12.6 to 1.1%, and CO selectivity remained higher than 99% at 1123 K under atmospheric pressure. Large amounts of unreacted molecular oxygen were detected in the eluted gas. The oxygen permeation flux of the membrane increased correspondingly from 1.89 to 2.1 ml/cm^2 min, which is only two times higher than that in air/He gradient. This is somehow different from our previous observations in a BSCFO membrane reactor using quartz tube, in which a high C_2 selectivity (48–73%) was achieved at different temperatures and different flow rates of diluted methane even though methane conversion was very low, typically 0.5–3.5% at 1073–1173 K. This may result from an oxidation of the produced methyl radicals or C_2 species to CO on the surface of the Ti-tube in the BSCFO membrane reactor.

The initial reaction during POM in the BSCFO membrane reactor is shown in Fig. 5. It can be seen that only 3–4 h are needed to initiate the membrane reaction, and then steady state is achieved. Methane conversion, CO selectivity and oxygen permeation flux are 46.7%, 80.6% and 8.3 ml/cm^2 min, respectively after 40 min of reaction. After 80 min of reaction, methane conversion, CO selectivity and oxygen permeation increased sharply to 91%, 92% and 13 ml/cm^2 min, respectively. After 3–4 h of reaction methane conversion, CO selectivity and oxygen permeation flux reached 92.2%, 90.3% and 15.5 ml/cm^2 min, respectively. Tsai et al. [10] reported results from POM in a dense disk-shaped $La_{0.2}Ba_{0.8}Co_{0.2}Fe_{0.8}O_{3-a}$ membrane reactor using 5% Ni/Al_2O_3 as a catalyst. They found that the oxygen permeation rate increased very slowly and reached its steady state only after 500 h. This might demonstrate that the BSCFO membrane adjusts itself more quickly to the new environment than a $La_{0.2}Ba_{0.8}Co_{0.2}Fe_{0.8}O_{3-a}$ membrane. In our previous study we obtained a shorter initial time for POM in the tubular BSCFO membrane reactor, and only one hour was needed to reach the steady state [24,25]. In addition, for a disk-type BCFZO membrane reactor, a similar and short initial time (about 1–2 h) was obtained [13]. Therefore, the initial reaction process of the membrane reactor for POM is closely dependent on the membrane reactor configuration, feeding mode, methane partial pressure, membrane material and the activation ability of the catalyst.

The effect of the air flow rate on the performance of the membrane reactor at 1123 K and 5 atm was investigated and is shown in Fig. 6. It can be seen that when the air feed rate increases from 100 to 250 ml/min, the oxygen permeation flux increases from 14.5 to 15.6 ml/cm^2 min. At the same time methane conversion increases from 86.8 to 92.4%, and the CO selectivity remains constant at about 90%. However, when the air flow got higher than 250 ml/min, there was almost no more influence on methane conversion, CO selectivity and oxygen permeation. In order to avoid a lack of oxygen supplied, the air flow rate was kept at 250 ml/min

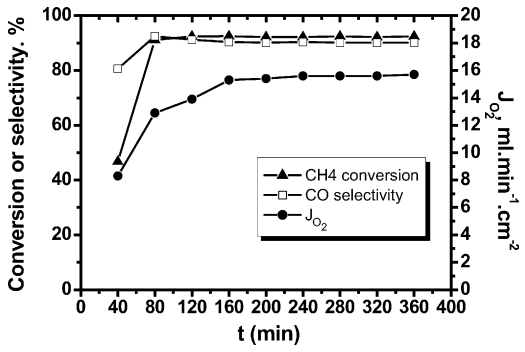

Fig. 5. The initial reaction stage of POM in the BSCFO membrane reactor at 1123 K and 5 atm.

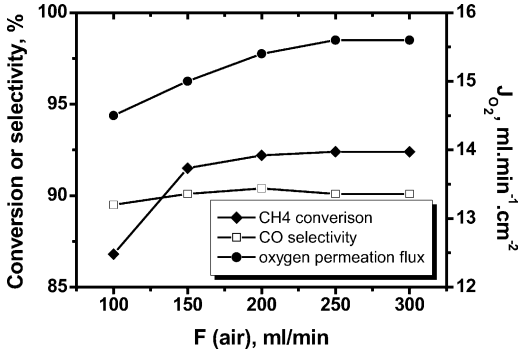

Fig. 6. Effect of air flow on the performance of the BSCFO membrane reactor at 1123 K and 5 atm.

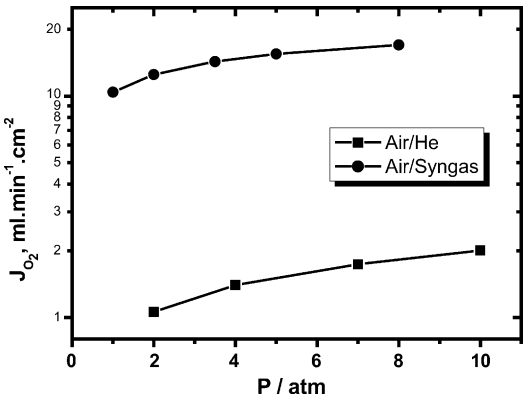

Fig. 7. Comparison of oxygen permeation fluxes through the BSCFO membrane under air/He and air/syngas gradients at 1123 K.

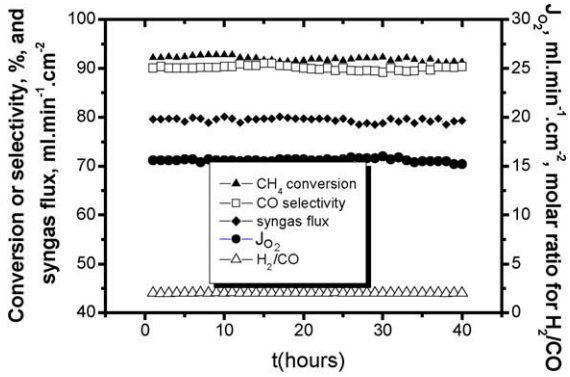

Fig. 8. Preliminary stability of the BSCFO membrane reactor at 1123 K and 5 atm.

or higher. Similar experiments demonstrated that, when the air flow rate was 200 ml/min or higher, the influence of the air flow rate on the oxygen permeation flux of the membrane reactor was negligible at 1123 K and constant pressure [2]. This shows that the exchange of oxygen on the membrane surface exposed to the oxygen rich side (air side) was not the controlling step of oxygen permeation with an air flow rate of 250 ml/min at 1123 K and 5 atm. Fig. 7 shows the total pressure dependence of the oxygen permeation flux under an air/He gradient and an air/syngas gradient in the BSCFO membrane reactor. It can be seen that the oxygen permeation flux in air/syngas was nearly one magnitude higher than that in air/He. In the air/He gradient, the oxygen partial pressure is 10^{-2} to 10^{-1} atm on the oxygen lean side, but under POM reaction conditions (air/syngas), the oxygen partial pressure could be as low as 10^{-19} atm [2,4]. The oxygen permeation flux increased from 10.5 to 17.0 ml/cm^2 min at 1123 K with changing pressure from 1 atm (constant pressure) to 8 atm under air/syngas gradient in the BSCFO membrane reactor. It can be seen that the oxygen permeance of BSCFO is improved significantly at high pressures. As reported previously, under POM conditions the surface-exchange kinetics become rate-limiting for the oxygen transport through the oxygen-permeable membrane [2,24]. Thus, with an increase of the oxygen partial pressure on the air side of the BSCFO membrane, the surface-exchange rate of oxygen ions increases correspondingly, which results in an improved oxygen permeability.

POM in the BSCFO membrane reactor was investigated previously under atmospheric pressure [4], high methane conversion (>98%), CO selectivity (>95%), and oxygen permeation flux (10.4 ml/cm^2 min) were obtained at 1123 K. Moreover, stable operation over long time (500 h) was achieved at 1148 K with a constant oxygen permeation flux of about 11.5 ml/cm^2 min, which demonstrated the excellent performance of the BSCFO membrane reactor. For practical application the membrane reactor should be operated at higher pressure. The preliminary results for high-pressure operation of the BSCFO membrane reactor are shown in Fig. 8. Over a period of 40 h 92% methane conversion, 90% CO selectivity and 15.5 ml/cm^2 min oxygen permeation flux were achieved in the BSCFO membrane reactor at 5 atm. These results demonstrate the feasibility of methane conversion to syngas in a BSCFO membrane reactor at higher pressure. Further investigations are underway. The SEM images of the membrane disk after reaction are shown in Fig. 9. Fig. 9a shows that the surface in contact with air was not eroded, but became loose which may have been caused by the frequent exchange of oxygen. However, the membrane surface in contact with syngas (Fig. 9b) was eroded significantly. A thin and highly porous carbonate layer (about 15 μm) was detected, moreover a few complex oxides were found by SEM–EDX. Below this layer, the bulk Perovskite structure was still maintained, which is confirmed

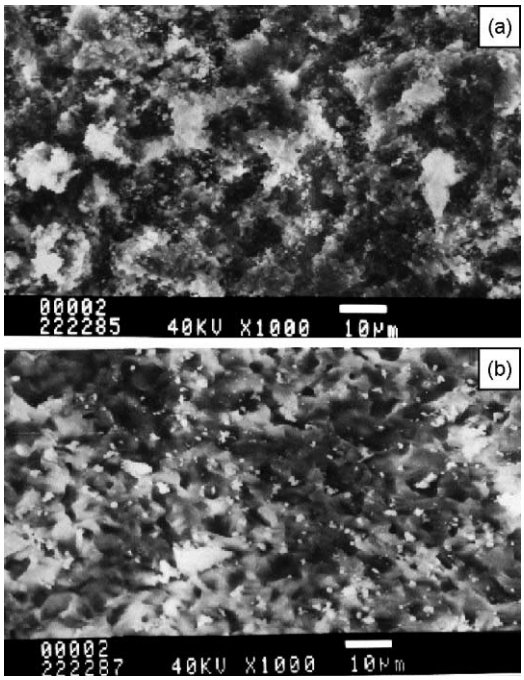

Fig. 9. SEM images of the surface morphology of the BSCFO membrane after POM. (a) Surface contacted with air, and (b) surface contacted with syngas/He.

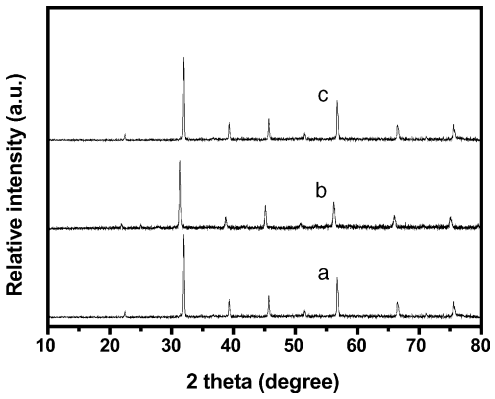

Fig. 10. XRD patterns of the BSCFO membrane disk after POM. (a) Fresh; (b) air side, unpolished; (c) syngas side, polished.

by XRD characterization of the membrane after reaction. As shown in Fig. 10, the Perovskite structure was preserved for the membrane surface in contact with the air side (unpolished), and for the polished surface in contact with the syngas side. It should be noted that only in a thin surface layer the perovskite structure was destroyed.

4. Conclusions

Oxygen-permeable $Ba_{0.5}Sr_{0.5}Co_{0.8}Fe_{0.2}O_{3-\delta}$ (BSCFO) membrane material was synthesized by the improved EDTA–citric acid complexation method. Oxygen permeation fluxes through dense disk-type BSCFO membranes were investigated at different temperatures (973–1123 K) and pressures (2–10 atm) under air/He gradient. A high oxygen permeation flux of 2.01 ml/cm^2 min for BSCFO was achieved at 1123 K at 10 atm under an air/He oxygen partial pressure gradient. The dependence of the oxygen permeation flux on the oxygen partial pressure gradient, $\ln(P_1/P_2)$, and the membrane thickness (L) suggests that the bulk diffusion was the rate-limiting step for oxygen transport across the BSCFO membrane under an air/He gradient. In addition, partial oxidation of methane (POM) to syngas ($LiLaNiO_x/\gamma$-Al_2O_3 as catalyst) in the BSCFO membrane reactor was performed successfully at high pressure (5 atm), and the BSCFO membrane reactor exhibited good stability for POM. Ninety-two percent methane conversion, 90% CO selectivity, and 15.5 ml/cm^2 min oxygen permeation flux were achieved in steady state at 1123 K and 5 atm. The XRD results show that the BSCFO membrane still preserved its cubic Perovskite structure in the bulk, demonstrating its high structural stability under POM reaction conditions.

Acknowledgements

The authors gratefully acknowledge financial support from the National Natural Science Foundation of China (Grant No. 50332040) and the Ministry of Science and Technology, PR China (Grant No. G1999022401).

References

[1] G.J. Hutchings, M.S. Scurrell, J.R. Woodhouse, Chem. Soc. Rev. 18 (1989) 251.
[2] H. Dong, Z.P. Shao, G.X. Xiong, J.H. Tong, S.S. Sheng, W.S. Yang, Catal. Today 67 (2001) 3.
[3] U. Balachandran, J.T. Dusek, S.M. Sweeney, R.B. Poeppel, R.L. Mieville, P.S. Maiya, M.S. Kleefisch, S. Pei, T.P. Kobylinski, C.A. Udovich, Am. Ceram. Soc. Bull. 74 (1995) 71.
[4] Z.P. Shao, H. Dong, G.X. Xiong, Y. Cong, W.S. Yang, J. Membr. Sci. 183 (2001) 181.
[5] J.E. ten Elshof, H.J.M. Bouwmeester, H. Verweij, Appl. Catal. A: Gen. 130 (1995) 195.
[6] Y. Lu, A.G. Dixon, W.R. Moser, Y.H. Ma, U. Balachandran, Catal. Today 56 (2000) 297.
[7] C.A. Udovich, Stud. Surf. Sci. Catal. 119 (1998) 417.
[8] E.P. Foster, P.J.A. Tijm, D.J. Bennett, Stud. Surf. Sci. Catal. 119 (1998) 867.
[9] U. Balachandran, J.T. Dusek, P.S. Maiya, B. Ma, R.L. Mieville, M.S. Kleefisch, C.A. Udovich, Catal. Today 36 (1997) 265.
[10] C. Tsai, A.G. Dixon, Y.H. Ma, AIChE J. 43 (1997) 2741.
[11] M. Schwartz, J. H. White, A. F. Sammels, US Patent 6,033,632 (2000).
[12] H.J.M. Bouwmeester, Catal. Today 82 (2003) 141.
[13] J.H. Tong, W.S. Yang, R. Cai, B.C. Zhu, L.W. Lin, Catal. Lett. 78 (2002) 129.
[14] S. Kim, Y.L. Yang, A.J. Jacobson, B. Abeles, Solid State Ionics 106 (1998) 189.
[15] T.H. Lee, Y.L. Yang, A.J. Jacobson, B. Abeles, M. Zhou, Solid State Ionics 100 (1997) 77.
[16] H. Kruidhof, H.J.M. Bouwmeester, R.H.E. van Doorn, A.J. Burggraaf, Solid State Ionics 63/65 (1993) 816.
[17] Y. Teraoka, T. Nobunaga, N. Yamazoe, Chem. Lett. (1988) 503.
[18] H.H. Wang, Y. Cong, W.S. Yang, J. Membr. Sci. 210 (2002) 259.
[19] X.F. Zhu, H.H. Wang, W.S. Yang, Chem. Commun. 9 (2004) 1130.
[20] L. Yang, Z.T. Wu, W.Q. Jin, N.P. Xu, Ind. Eng. Chem. Res. 43 (2004) 2747.
[21] B.C.H. Steele, Mater. Sci. Eng. B13 (1992) 179.
[22] B.C.H. Steele, Curr. Opin. Solid State Mater. Sci. 1 (1996) 684.
[23] C. Wagner, Z. Phys. Chem. B21 (1933) 25.
[24] H.H. Wang, Ph.D. Thesis, Dalian Institute of Chemical Physics, Chinese Academy of Science, 2003, p. 37, p. 55.
[25] H.H. Wang, Y. Cong, W.S. Yang, Catal. Today 82 (2003) 157.